ISSN 1990-3413, Astrophysical Bulletin, 2016, Vol. 71, No. 2, pp. 232–240. © Pleiades Publishing, Ltd., 2016.
Original Russian Text © N.G Peterova, N.A. Topchilo, 2016, published in Astrofizicheskii Byulleten', 2016, Vol. 71, No. 2, pp. 251–260.

The Gelfreikh–Lubyshev Effect according to Microwave Observations of Sunspots

N. G. Peterova[1*] and N. A. Topchilo[2]

[1] *St. Petersburg Branch of the Special Astrophysical Observatory of the Russian Academy of Sciences, St. Petersburg, Russia 196140*

[2] *St. Petersburg State University, St. Petersburg, 199034 Russia*

Received October 5, 2015; in final form, February 25, 2016

Abstract—We report the results of RATAN-600 radio telescope observations of the fine structure of the source of cyclotron microwave emission (SCMR) located in the solar corona above the main sunspot of NOAA 11899 active region. Compared to earlier and mostly episodic observations of the SCMR, our regular observations with RATAN-600 radio telescope showed rather conclusively that the variation of the structure of the SCMR as a function of the angle of view in the present case is of geometric nature. The behavior of image variations generally agree with the computations performed by Gelfreikh and Lubyshev in terms of the simplest model of the solar atmosphere above the sunspot. The results of their computations are widely used for interpreting observations.

DOI: 10.1134/S1990341316020103

Keywords: *sunspots—Sun:radio radiation—Sun:magnetic topology—Sun:atmosphere*

1. INTRODUCTION

Sunspots, where strong magnetic fields (2–4 kG) emerge from under the photosphere into the corona, are observed on the solar disk at radio frequencies as the brightest features of the microwave emission source located above quasi-quiescent (outside flares) active regions. The main generation mechanism of this emission is believed to be cyclotron mechanism at low (mostly second and third) harmonics of the gyrofrequency [1]. The observed spectrum of sunspot fluxes, their brightness temperature and polarization degree are determined by the steep, two orders of magnitude, increase of electron temperature above the sunspot from chromospheric to coronal values (2–4 MK), and by the decrease of magnetic-field strength with height. Because of the strong dependence of optical depth on the angle between the line of sight and magnetic-field direction, the SCMR image should vary strongly depending on the position of the sunspot on the solar disk [2]. In the process, small-scale features may appear, which can be found only in observations made with a high resolution (one arc second or better). To validate our concepts about the nature of SCMR emission and refine the physical parameters of hot coronal plasma in the presence of a strong magnetic field, we need a detailed comparison of model computations with high-precision observations made with high spatial resolution.

Fine features of the SCMR image were first noted during 4.5-cm observations of the March 7, 1970 solar eclipse [3]. A bright, approximately 4″-wide fringe with close to 100% circular polarization degree was found at the boundary of a large sunspot. The formation of such features was evident from the cyclotron emission theory for SCMR [2], however, with the advent of large interferometers it became necessary to perform more detailed computations of *two-dimensional* SCMR images. Gelfreikh and Lubyshev [4] performed such computations in terms of simplified concepts about both the structure of magnetic field emerging into the corona, and about the height distribution of temperature and density. It was shown that model SCMR images in the sky plane have the form of a ring or a crescent that change their shape depending on the position of the sunspot on the solar disk (we propose to call this phenomenon the Gelfreikh–Lubyshev (G–L) effect). Similar results were later obtained by [5], who computed coronal magnetic field by extrapolating actually measured photospheric magnetic fields.

The high angular resolution of microwave observations, which is necessary to see the fine structure of the SCMR image, is achieved during observations of solar eclipses or by using synthetic-aperture telescopes such as WSRT, VLA, and OVRO. The above

*E-mail: peterova@yandex.ru

instruments were used to observe sufficient number (about 50) of active regions in the 2–20 cm wavelength interval ([6–11], etc). Most of the results were obtained with a resolution of 2″–4″ in interferometric observations and somewhat poorer resolution of 4″–6″ in solar-eclipse observations. In many cases such observations revealed the ring- or horseshoe-shaped structure of the observed brightness temperature distribution, with and without brightness depressions above sunspot umbrae. These structures were most often interpreted as manifestations of the G–L effect. However, this conclusion remained insufficiently substantiated because of the episodic nature and short duration of such observations, which could not explicitly reveal the dynamics of the G–L effect. This may explain why some authors propose, from time to time, other interpretations of the peculiarities of observed SCMR images in terms of complex models of sunspot magnetic fields and temperature and density distributions above them [10–12].

During the epoch of moderate-resolution (1′–3′) observations geometric effects were investigated in terms of the radiation directivity analysis. In particular, one such a study [13] preceded the work of [4]. Regular observations with somewhat higher angular resolution (10″–20″) made with Nobeyama radio heliograph (NoRH) and Siberian Solar Radio Telescope were used to study the directivity of SCMR emission. In one of the cases [14] they revealed geometric variations of maximum brightness—the brightness at the short 1.76 cm wavelength is minimal when the sunspot is located at the central solar meridian and symmetrically increases (by a about a factor of three) when the sunspot approaches the E–W limbs. This result can be interpreted as a manifestation of the G–L effect, however, for such interpretation to be sufficiently conclusive, it would be necessary to describe and analyze the shift of the emission center relative to the geometric sunspot center.

In this paper we report a study specially dedicated to the investigation of the G–L effect for the case of a particular sunspot using observations that make it possible to follow the entire cycle of the variations of the SCMR image from the rise of the active region to its disappearance behind the solar limb. The current solar cycle is distinguished by large number of sunspots that can be considered to have regular (circular) shape and therefore more suitable for searching for and analysis of the manifestations of the G–L effect. We chose the active region NOAA 11899 (November, 2013), which actually consisted of a single large sunspot and, what is important for the comparison, passed almost through the center of the solar disk, where the G–L effect should show up with the highest contrast.

2. DESCRIPTION OF THE ACTIVE REGION NOAA 11899

Active region NOAA 11899 (latitude $\varphi = 4–7°$N, the CMP—the time of the central solar meridian passage—18.11.2013) was distinguished by stability and simple morphological and magnetic structure (class C-D-H and $\alpha–\beta$, respectively). On the photoheliogram (see Figs. 1 and 3) it appears as a single sunspot of southern (S) polarity and almost of regular shape, which at the CMP had the penumbral size of about 80″. According to ground-based and satellite observations the total area of the sunspot (umbra+penumbra), which was equal to 745 ± 30 msh (1 msh $= 10^{-6} S_\odot$, where $S_\odot$ is the area of the hemisphere), and its morphology varied only slightly (see Fig. 1 and the table).

The choice of the Active Region (AR) 11899 as an object to investigate the G–L effect was due to its position on the solar disk—the region was located at low latitude ($\varphi = 4–7°$N) and, the solar north pole at that time was conveniently tilted in the Earth direction ($b \approx 2.5°$ at the CPM). Because of this circumstance the minimum angular distance between the sunspot umbra and the disk center (i.e., angle of view θ) was as small as 3.25°. The closest approach occurred at 16:06 UT on 18.11.2013. The closest radio observations in time were those performed on RATAN-600 ($\theta \approx 5°$, see the table).

Magnetic field varied only slightly in the process of the sunspot passage across the solar disk. The flare activity of NOAA 11899 was weak and ended before the group crossed the central meridian. Another favorable circumstance consisted in the fact that AR 11899 was well isolated from the neighboring active regions (see inset frames in Fig. 1), which is important for the analysis of observations performed with one-dimensional angular resolution, like those carried out on RATAN-600 and serve as the basis for this study.

On the whole, the above properties of AR 11899 allow us to view it as a stable sunspot (at least during the CMP) and associate the dynamics of its SCMR described below with then manifestation of specific directivity of emission (the G–L effect).

3. OBSERVATIONS, THEIR REDUCTION, AND RESULTS

In this study we used the data of regular standard solar spectropolarimetric observations performed on RATAN-600 radio telescope and downloaded from the archive of the Radio-Astronomical Center of the Solar Activity Forecast[1]. Beginning with 2011, the

[1] http://www.spbf.sao.ru/prognoz/

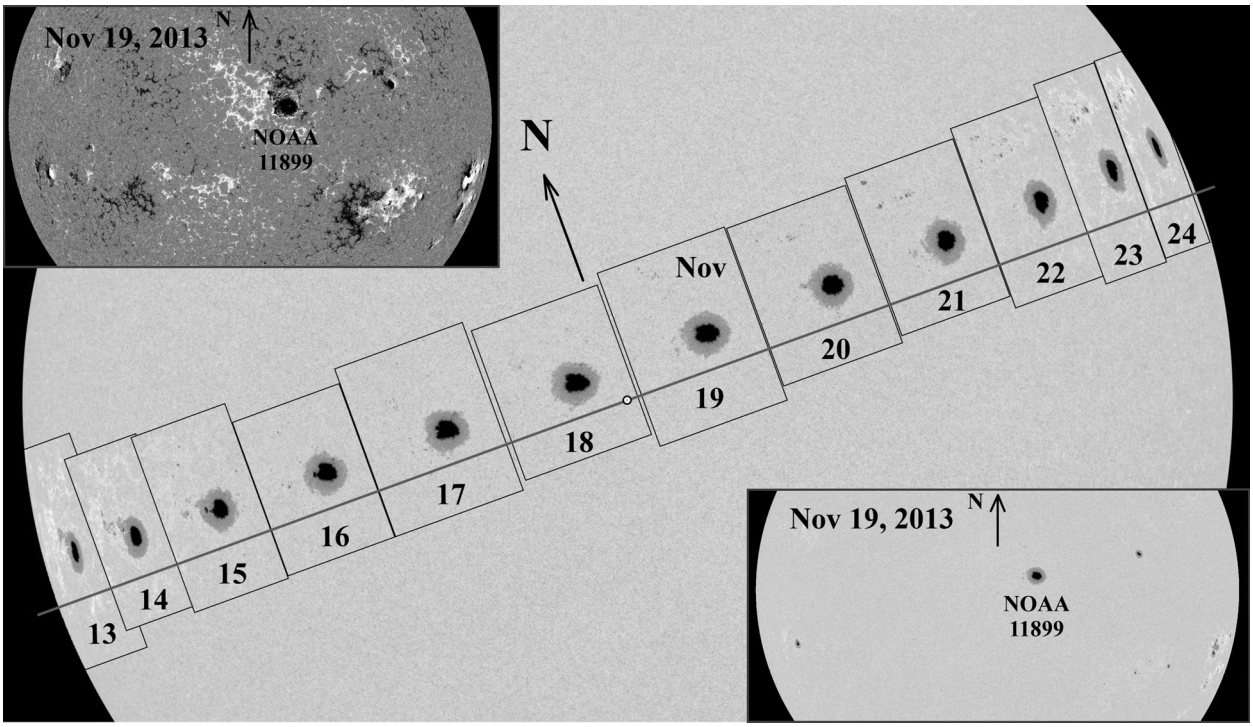

Fig. 1. Shape and position of a sunspot in the NOAA 11899 group at the RATAN-600 observing times over the entire period while the group remains at the solar disk from November, 13 and 24, 2013 (the dates are given at the bottom). The open circle shows the position of the solar disk center. The inset figures at the top left and bottom right show the magnetogram and photoheliogram of the solar-activity belts for Nov, 13, 2013 according to SDO/HMI.

frequency resolution of RATAN-600 instruments was improved to 1% [16], allowing detailed study of spectral properties of active regions. We used standard reduction algorithm to analyze observations. The best one-dimensional angular resolution of RATAN-600 is 14″, and it degrades in proportion with wavelength amounting to about 40″ in the middle part of the wavelength interval (at 5 cm). The reported results of observations refer to the time of local solar culmination (about 8:59 UT). We used the data from SDO (HMI and AIA instruments) and HINODE (SOT/SP) observatories at the times maximally close to those of RATAN-600 observations (the time difference with SDO observing time was typically less than 1 minute) as additional data.

The radio spectra obtained on RATAN-600 (see Fig. 2) exhibit a pattern typical of cyclotron emission of sunspots: the flux rapidly increases in the 2–5 cm wavelength interval and polarization at short wavelengths is close to 100%, and decreases with further increase of wavelength. The form of the spectrum is stable, showing only minor dynamics, which is possibly due to variations of the total area and magnetic field of the sunspot.

According to RATAN-600 data, the image of the SCMR of the compact but not highly fragmented sunspot has the form of a smooth curve resembling a Gaussian. The SCMR preserves such a form from the longest wavelengths, where it is determined by the beam pattern, down to the shortest wavelengths, where the magnetic field strength still allows the generation of cyclotron emission. Although for the great sunspots the angular resolution of RATAN-600

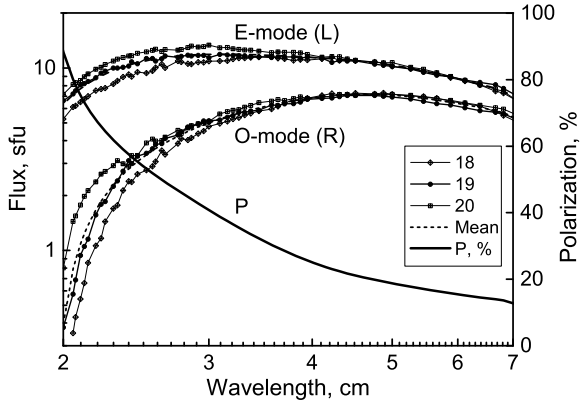

Fig. 2. SCMR flux spectra of a sunspot in NOAA 11899 during its central meridian passage on 18–20.11.2013 according to RATAN-600 radio-telescope observations separately in both modes (E and O). Mean are the mean fluxes for E- and O-modes averaged over these three days and P is the polarization degree spectrum computed using these values.

Table. Dynamics of the area (Sp), magnetic-field strength (B), and angle of view (θ) of the leading sunspot of NOAA 11899 group

Date, 2013	Sp, msh [1] Debrec. Ground	Sp, msh [1] Debrec. SDO/HDI	B, Gs [2] CRAO	B, Gs [3] SDO/HDI	B, Gs [4] Hinode	$\theta_{\rm Nob}$, °	$\theta_{\rm Ratan}$, °	Flares, GOES
	$\sim 0^{\rm h}$	$8^{\rm h}\ 59^{\rm m}$	$0–9^{\rm h}$	$0^{\rm h}$ UT	$\sim 12^{\rm h}$	$2^{\rm h}\ 44^{\rm m}$	$8^{\rm h}\ 59^{\rm m}$	
15.11	765	771	2800	3750	–	47.7	44.3	M1.0
16.11	762	718	2500	3840	–	34.3	30.9	–
17.11	706	674	–	3910	–	20.9	17.5	C1.7
18.11	721	725	–	3710	–	8.0	5.1	–
19.11	813	724	–	3690	4190	6.8	10.0	–
20.11	755	728	3200	3570	4340	19.5	22.9	–
21.11	801	765	–	3560	4250	32.7	36.2	–
22.11	748	752	–	3500	4080	46.1	49.1	–

[1] According to the data from Debrecen observatory (http://fenyi.solarobs.unideb.hu/deb_obs_en.html) [15].
[2] According to measurements made at Crimean Astrophysical Observatory (http://solar.crao.crimea.ua/data/sunspots/).
[3] Maximum magnetic field strength in the sunspot umbra that we computed based on original SDO/HMI maps of the full magnetic field vector (http://jsoc.stanford.edu/ajax/exportdata2.html), smoothed to educe instrumental noise.
[4] Same for HINODE data (http://www.csac.hao.ucar.edu/csac/archive.jsp#Hinode).

at short wavelengths is sufficient to image the fine structure, in most of the cases only the size of the source varies whereas its shape remains the same. However, in the case of AR 11899, despite the circular symmetry of the sunspot observations show the fine structure of its image, which undergoes significant and rapid changes.

Figure 3 shows the entire set of RATAN-600 SCMR scans in the 1.65–10 cm wavelength interval taken over three days near the time of the central meridian passage, when the variations of the fine structure are most appreciable (see [17] for details). As is evident from the figure, the fine structure of the image is absent at long wavelengths, possibly due to insufficient angular resolution of RATAN-600.

The fine structure of the image and its variations show up most conspicuously at short wavelengths, as can be seen in a zoomed-in scale in Fig. 4, where we show the variations of the image structure over six observing days. It is evident from the figure that the fine structure of the image near the CMP varies strongly with angle of view (observing angles $\theta_{\rm Ratan}$ are listed in the table). On the day when the angle of view at the time of observation ($\theta \approx 5°$) was closest to the minimum value (19.11.2013), the SCMR image has a symmetric, "two-humped" structure, which is indicative of strong darkening in the central part of the sunspot. The symmetry disappears on the neighboring days (18.11 and 20.11) and the outer edge of the SCMR, which was shifted toward the solar E-limb when the sunspot was located in the eastern hemisphere of the Sun (18.11.2013) and toward the W-limb when the sunspot was located in the western hemisphere (20.11.2013). The E–W asymmetry direction remains unchanged in both hemispheres with further increase of the angle of view, however, the asymmetry degree rapidly decreases and the source acquires its "standard" symmetric form. The fine structure and asymmetry appear smeared at long wavelengths because of the degraded angular resolution of RATAN-600 and perspective SCMR size decrease when the sunspot approaches the limb.

The 2D images shown in Fig. 3 based on 1.76 cm data of the Nobeyama radio heliograph confirm our results obtained with RATAN-600. It is evident from a comparison of the NoRH image of the sunspot (the fourth row of figures from the top) with shorter-wavelength RATAN scans (the lower curves in the top row of figures) that the brightness maximum in E-mode NoRH images shifts with time from left to right relative to the optical sunspot image in the same way as the E-mode signal maximum in RATAN scans. A

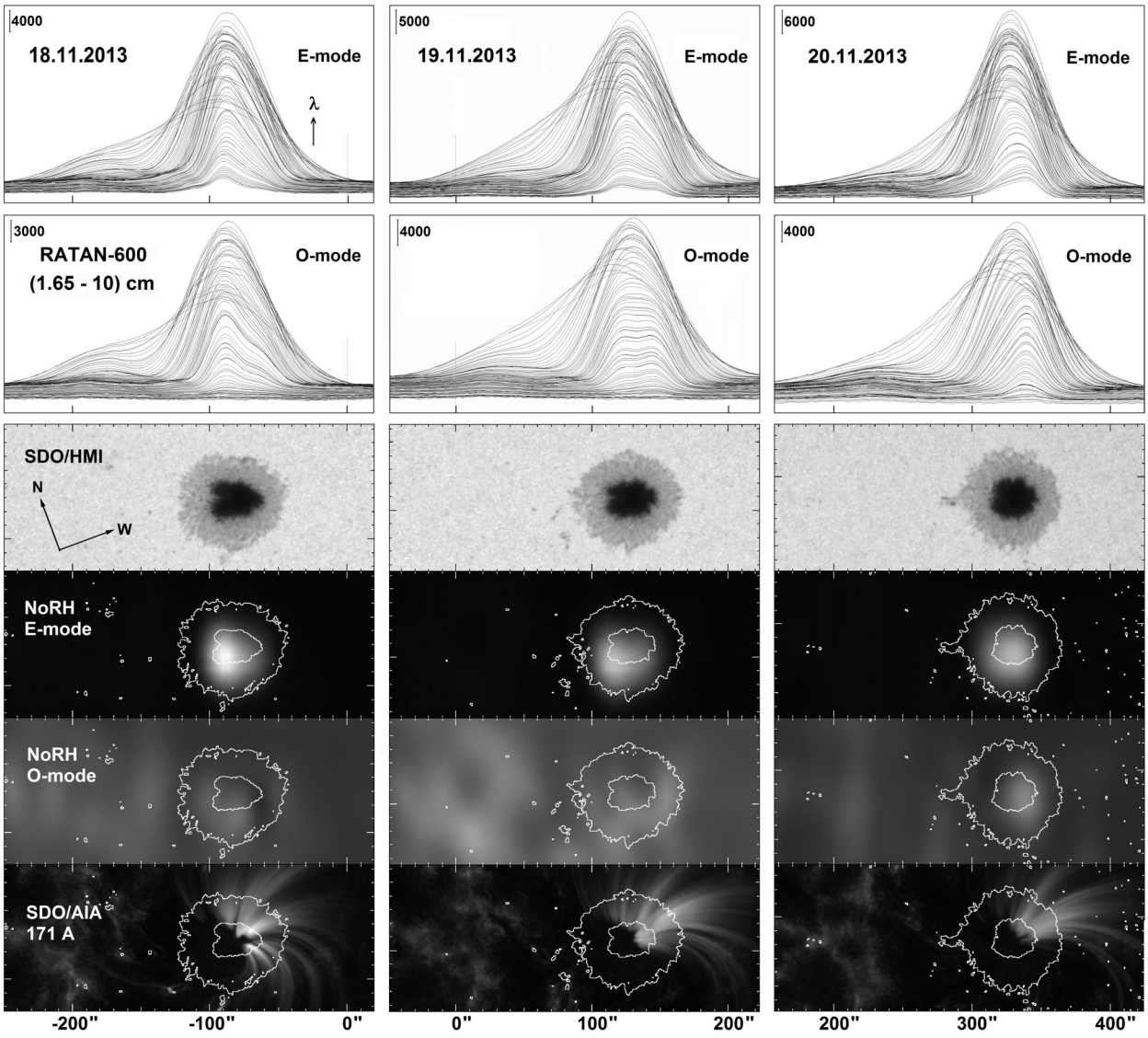

Fig. 3. The 1.65–10 cm RATAN-600 scans of NOAA 11899 taken over three days (18–20.11.2013) near the CMP time shown separately in the E- and O-modes. The arrow with the λ sign indicates the direction of the wavelength increasing, and the thin vertical lines indicate the passage of the telescope beam across the solar disk center. The scans are displayed in the antenna temperature scale. RATAN-600 observations are compared to SDO/HMI data—the photoheliogram and UV sunspot image in the 171 Å line—and to observations made with Nobeyama radio heliograph in the E- and O-modes. The white contours in the maps show the boundary between the sunspot umbra and penumbra. The map scales are in arcseconds along both axes, which are in the Cartesian coordinate system rotated by the inclination of the solar rotation axis (see Fig. 1).

similar shift can also be seen in the O-mode NoRH data (the second to last rows of figures), however, it is less significant because of the weakness of the signal in this mode (the sunspot polarization degree in NoRH and short-wavelength RATAN-600 data is close to 100%).

An analysis of the images shown in Fig. 3 also leads us to conclude that the fine structure of the radio image reported here is not associated with the activity in the sunspot. Thus according to SDO/AIA data although the loops seen in the UV somewhat change their intensity, they nevertheless maintain their position in the western part of the sunspot and cannot be the cause of the observed radical change of the source asymmetry direction.

4. DISCUSSION

The G–L model [4] was developed for a source of cyclotron emission. Observations described in Section 3 confirm that the the radio source above the sunspot in NOAA 11899 was indeed a typical cyclotron sunspot source (see Fig. 2), and a sufficiently stable one.

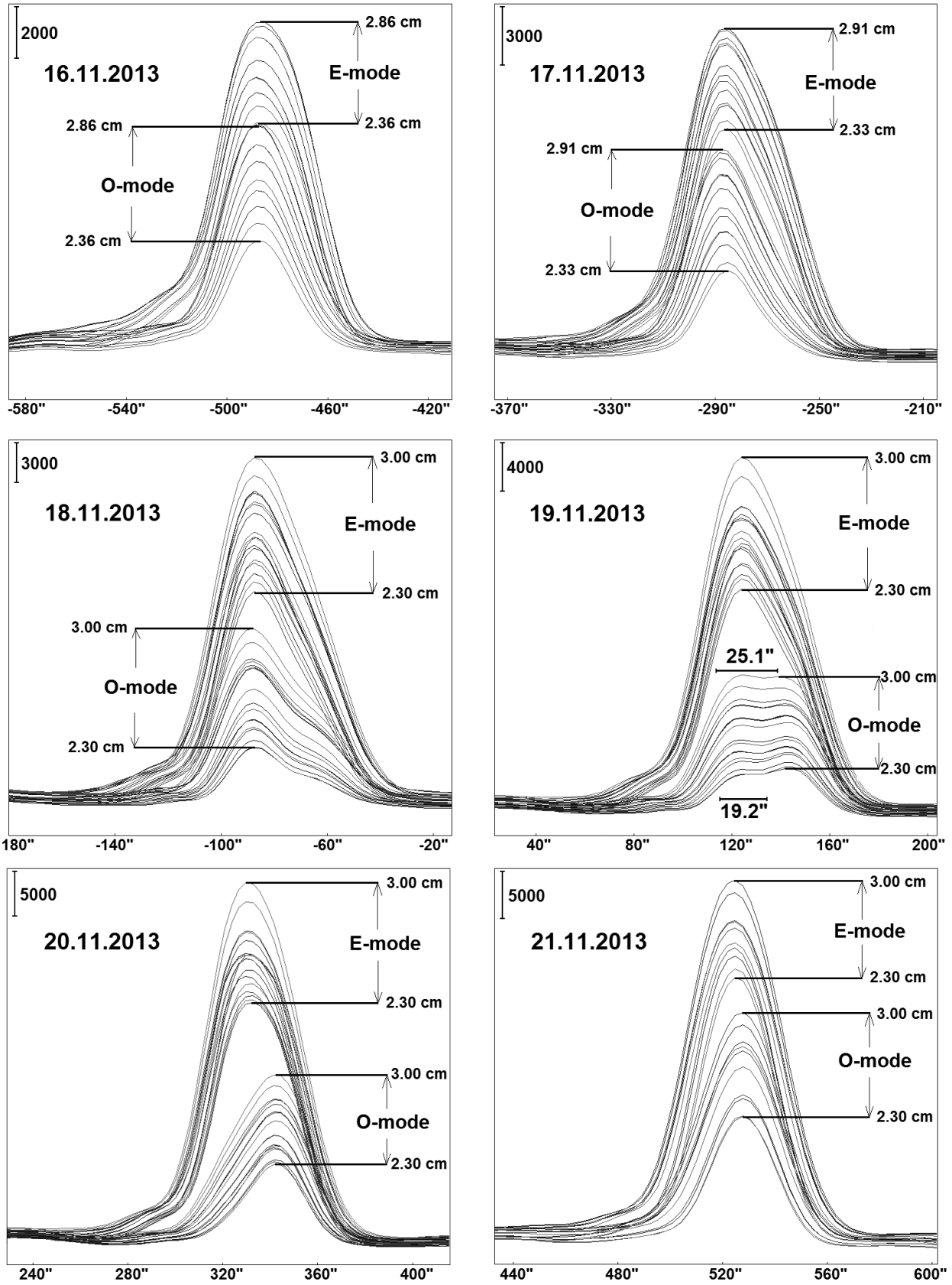

Fig. 4. The 2.3–3.0 cm RATAN scans of NOAA 11899 according to six-day observation data 16–21.11.2013. The scans are shown in the antenna temperature scale. We show in the 19.11.2013 frame the size of the RATAN-600 beam pattern at the extreme wavelengths: 19″.2 at 2.30 cm and 25″.1 at 3.00 cm.

A characteristic feature of the fine structure of the observed source image—the brightness depression above the sunspot center, which had the highest contrast in O-mode, showed up conspicuously in the case considered, as expected according to the SCMR theory [2]. Another feature demonstrated by observations consists in the asymmetry of scans, which increases with increasing distance from the center of the Sun. Both features are completely qualitatively consistent with the model 2D sunspot images computed by [4], and this fact is indicative of the fundamental adequacy of the model employed. Note that the peculiarities of the dynamics of the variations of the sunspot image structure pointed out in this study were revealed solely because of the regular nature of RATAN-600 observations covering a wide range of wavelengths and performed with high frequency resolution of the receiving equipment [16].

Validating the feasibility of the G–L model as a specific *physical model* of the atmospheric structure above the sunspot requires either direct observations of characteristic two-dimensional structures (crescents/rings) or detailed numerical computations showing the influence of two-dimensional structures on the observed one-dimensional cross sections/scans. In this case *the dynamics* of the change of the sunspot image as it moves across the solar disk can serve as an argument in favor of some model atmosphere.

The paper by Lee et al. [9] stands out among many earlier studies citing [4], and it makes sense to compare their results with ours. It is the only study specially dedicated to the search for the G–L effect, performed over a wide range of wavelengths based on spectropolarimetric observations of the sunspot in NOAA 4741 (August, 1986), which—and this is very important—passed through the center of the solar disk (like in the case of NOAA 11899). The spot was small with its area, penumbra size, and maximum magnetic-field strength equal to 200–250 msh, about 35″, and about 2400 *G*, respectively. Observations were made with OVRO interferometer in the 4–12 GHz frequency interval practically in one-dimensional mode with a resolution 6.″8–2.″2, which is higher than that of RATAN-600 observations. Unlike our study, [9] could trace only the second half of the active region's passage across the solar disk, from the center to the western disk edge (see Fig. 5a).

A comparison of observations shows that the fine structure of the sunspot image obtained with RATAN-600 shows up clearly in the 2–3 cm wavelength interval (see Fig. 4), whereas in the case of OVRO observations it shows up at longer wavelengths, starting from 3.6 cm,—and is not so clearly defined. The difference between the images obtained at short wavelengths is primarily due to different sunspot sizes and different magnetic field strength (3200 and 2400 G in NOAA 11899 and NOAA 4741, respectively, according to the data obtained at Crimean Astrophysical Observatory). The difference in the structure observed at long wavelengths can be explained by insufficiently high resolution of RATAN-600, which is confirmed, e.g., by eclipse observations of the sunspot in NOAA 11140 (the sunspot area and its distance from the solar disk center were equal to about 180 msh and 40° respectively, in January 2011) performed with RT-32 radio telescopes of the Institute of Applied Astronomy of the Russian Academy of Sciences at 3.5 and 6.2 cm with a very high angular resolution of about 1″ [18], where the SCMR image (see Fig. 5b) at both wavelengths had a "two-humped" structure and asymmetry typical of the G–L effect (Fig. 5c).

As a result, optimally chosen data reveal an observational fact that conclusively confirms that the effects predicted by the G–L model (even despite its simplified nature) exist and manifest themselves in the modifications of the SCMR image and shifts of the emission center in line with this model. To directly reveal the two-dimensional fine structure of the image (rings, crescents) typical for SCMR, higher angular resolution is needed, 2″–4″, which is so far unachievable in regular solar observations.

Studies of the G–L effect are important because they contribute both to the development of the technique of sunspot observations and to investigation of the physical parameters of coronal plasma above sunspots. One of the most challenging tasks in the studies of SCMR is the measurement of its height above the photosphere level, which is measured from the shift of the SCMR emission center relative to the geometric center of the sunspot. The technique of these measurements should take into account the fact that both effects (height and angle of view) have qualitatively the same effect on the offset of the emission center by shifting it toward the limb. The height effect is comparable to the G–L effect at large angles of view, whereas the interfering G–L effect is much stronger at small angles of view. This can result in a significant overestimation of the results of SCMR height measurements, especially when they are based on observations in the central part of the solar disk as earlier point out by [2]. For example, in the case of NOAA 11140 (see Fig. 5c) the SCMR emission center is offset by about 10″ toward the limb relative to the geometric sunspot center. If the G–L effect is not taken into account the error of measured height may amount to 100%.

In conclusion we, like [5], emphasize that the G–L effect is determined solely by the dependence of the optical depth of the microwave emission source above the sunspot on the angle of view at which it is

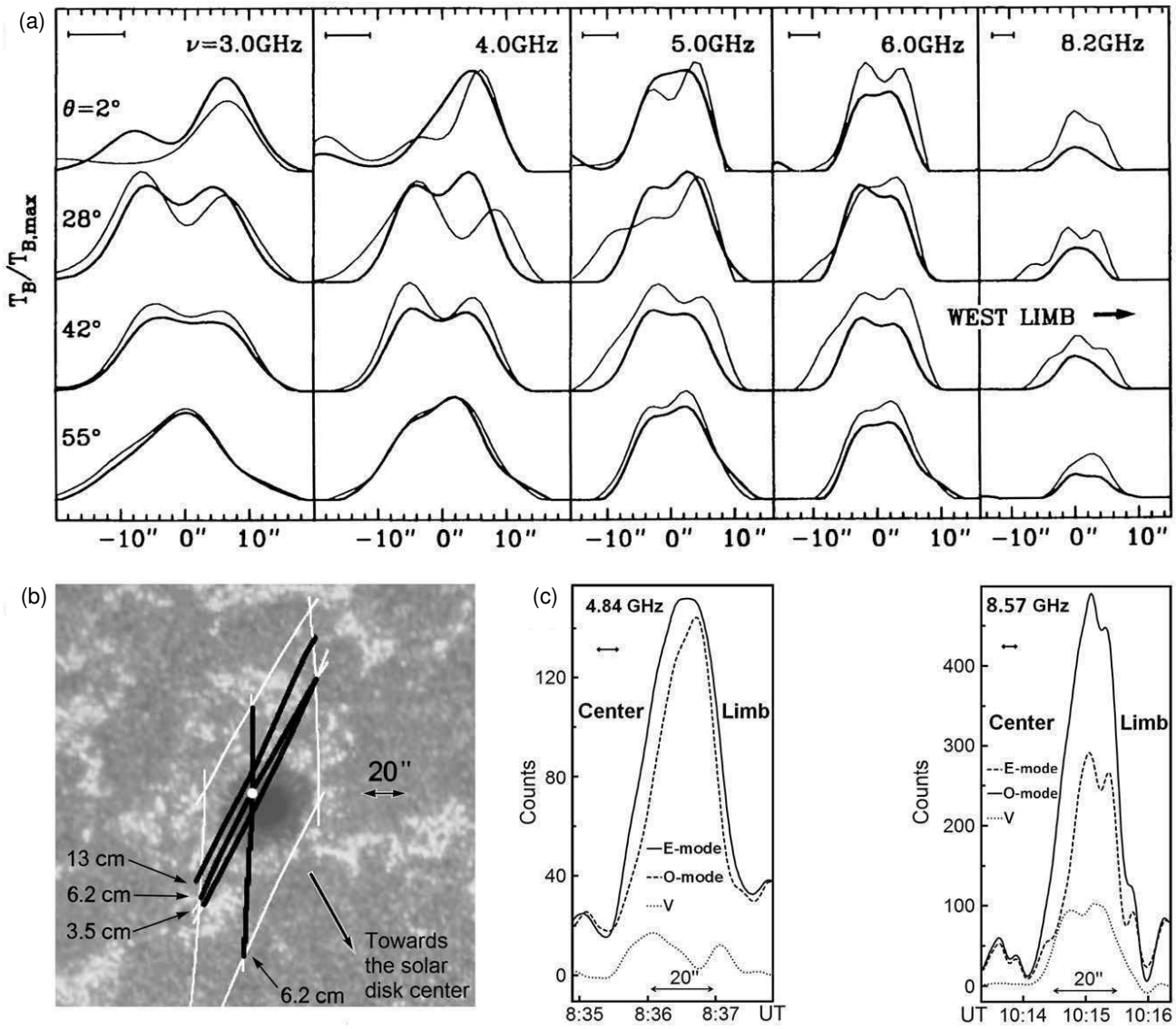

Fig. 5. Comparison of the fine structure of SCMR based on observations made with different instruments: (a) OVRO scans of NOAA 4741 in the 3–8.2 GHz frequency interval for angles of view 2°–55° in both emission modes (E-mode — the thin line and O-mode, the thick line) adopted from [9]; (b) photoheliogram of AR 11140, where we indicate the positions of the maxima of one-dimensional brightness distributions at three wavelengths (black lines) and the position of the mass center of SCMR emission at 6.2 cm (the white dot) according to observations of the January 4, 2011 solar eclipse made with RT-32 telescope of the Institute of Applied Astronomy of the Russian Academy of Sciences [18]; (c) one-dimensional distribution of SCMR brightness above the sunspot in NOAA 11140 during the eclipse at two frequencies (3.5 and 6.2 cm) close to the frequencies of OVRO observations. The "Center" and "Limb" captions indicate the source edges closest to the center and limb of the solar disk, respectively. The angular resolution is indicated at the top left for all scans and for scans made at the time of eclipse was chosen close to the OVRO resolution .

observed. The structural features of SCMR (rings) found in observations should be by no means viewed as conclusive evidence for the existence of local small-scale high-temperature plasma sources in the sunspot without first verifying them for manifestations of the G–L effect.

On the other hand, there are a number of undoubted cases where apparently similar structures (rings/crescents) are observed, which, however, are not due to the G–L effect [12]. Their main visible difference is that in these cases the brightness maximum may be located anywhere in the sunspot, whereas in the case of the G–L effect it should always be offset away from the solar disk center. [11] showed that in this case the actual plasma parameters differ so much from their simplified model values that this difference masks the G–L effect thereby explaining the difficulty

and rareness of observations of this effect in its "pure" form like in the case of NOAA 11899.

5. CONCLUSIONS

(1) We report for the first time the results of observations that confirm very conclusively the significant specific effect of angle of view on sunspot images when observed at microwave frequencies, which manifests itself in the appearance of ring- and crescent-shaped structures in the image. We propose to call this phenomenon the Gel'freikh–Lubyshev effect by the names of two researchers who were the first (in 1979) to compute the now highly popular two-dimensional model of the phenomenon.

(2) We demonstrate the advantages of observing the G–L effect at microwave frequencies, where it shows up most contrastively because the sharp temperature gradient.

(3) We point out that the G–L effect should always be taken into account in the measurements of the height of the cyclotron source lying in the corona above the sunspot.

ACKNOWLEDGMENTS

We are grateful to RATAN-600 team for sharing the results of solar observations in public domain, and also to the other teams whose observational data we used in addition to RATAN-600 data to interpret radio observations: Debrecen Heliophysical Observatory (DHO). The RATAN-600 radio-telescope observations were carried out with the financial support of the Ministry of Education and Science of the Russian Federation (state contract 14.518.11.7054, code 2012-1.8-16-518-005). The SDO/HMI data and images were kindly provided by NASA/SDO and AIA, EVE, and HMI research teams. HINODE is a Japanese mission developed and launched by ISAS/JAXA, collaborating with NAOJ, NASA and STFC (UK) as international partners. The mission is operated by the above organizations collaborating with ESA and NSC (Norway). We are especially grateful to the team of Nobeyama Radio Heliograph operated by NAOJ/Nobeyama Solar Radio Observatory for the excellent quality of the data provided.

REFERENCES

1. V. V. Zheleznyakov, *Radio emission of the Sun and planets* (Pergamon Press, Oxford, New York, 1969).
2. E. Ya. Zlotnik, Sov. Astron. **12** (2), 245 (1968); **12** (3), 464 (1968).
3. J. A. Quiñones, A. N. Korzhavin, N. G. Peterova, and J. Santos, Byulletin Solnechnye Dannye Akademie Nauk USSR **1975**, 87 (1975).
4. G. B. Gel'freikh and B. I. Lubyshev, Sov. Astron. **23** (3), 316 (1979).
5. J. Hildebrandt, N. Seehafer, and A. Krüger, Astron. and Astrophys. **134**, 185 (1984).
6. K. R. Lang and R. F. Willson, Astrophys. J. **255**, L111 (1982).
7. C. E. Alissandrakis and M. R. Kundu, Astrophys. J. **253**, L49 (1982).
8. D. McConnel and M. R. Kundu, Astrophys. J. **279**, 421 (1984).
9. J. W. Lee, D. E. Gary, and G. J. Hurford, Solar Phys. **144**, 349 (1993).
10. A. Vourlidas, T. S. Bastian, and M. J. Aschwanden, Astrophys. J. **489**, 403 (1997).
11. E. Ya. Zlotnik, S. M. White, and M. R. Kundu, ASP Conf. Ser. **155**, 135 (1998).
12. C. E. Alissandrakis and M. R. Kundu, Astron. and Astrophys. **139**, 271 (1984).
13. B. I. Lubyshev, Sov. Astron. **21** (1), 74 (1977).
14. I. A. Bakunina, G. Ya. Smolkov, and S. D. Snegirev, Radiophysics and Quantum Electronics **51** (8), 579 (2008).
15. L. Györi, T. Baranyi, and A. Ludmány, IAU Symp, **273**, 403 (2011).
16. V. M. Bogod, A. M. Alesin, and A. A. Pervakov, Astrophysical Bulletin **66** (2), 205 (2011).
17. N. A. Topchilo, N. G. Peterova, in *Proceedings of the XVIII All-Russian Annual Conference "Solar and Solar-Terrestrial Physics — 2014"*, Edited by A. V. Stepanov, Yu. A. Nagovitsin (Main (Pulkovo) Astronomical Observatory of the Russian Academy of Sciences, St.-Petersburg, 2014), p. 419.
18. A. N. Korzhavin, N. G. Peterova, and N. A. Topchilo, Geomagn. Aeron. **52** (7), 867 (2012).

Translated by A. Dambis